Geografia Fisica e Dinamica Quaternaria
GFDQ 49 (2026), 227-244

DOI 10.4454/j3c5gh52

Qutbudin ISHANCH[1*], Sharon PITTAU[2], Giovanni MONEGATO[3], Vittoria SCORPIO[2], Kanchan MISHRA[1], Tobias LAUER[1], Christiane ZARFL[1], Kathryn E. FITZSIMMONS[4]

Sedimentary characteristics of fluvial deposits from the Serio River, northern Italy: implications for recent channel evolution

Abstract: Ishanch Q., Pittau S., Monegato G., Scorpio V., Mishra K., Lauer T., Zarfl C., Fitzsimmons K.E., *Sedimentary characteristics of fluvial deposits from the Serio River, northern Italy: Implications for Recent Channel Evolution.* (IT ISSN 0391-9838, 2026). This study investigates fluvial sediments from the Serio River in the southern Alps of northern Italy to evaluate how source lithology, sediment transport, depositional processes, and anthropogenic modification influence sediment characteristics and recent channel evolution. Grain size, sand composition, and geochemical analyses from mountain valley and piedmont plain depositional contexts pronounced spatial and vertical variations in sediment properties. The Serio River, which is heavily regulated, exhibits strong spatial and vertical variability in sediment properties, with heterogeneous grain-size distributions and sediment compositions. Channel bank profiles record a transition from older, coarser, lithic-rich sediments at depth, to younger, finer, more carbonate-rich deposits near the surface, reflecting channel incision, lateral migration, and overbank deposition. Geochemical and petrographic evidence further demonstrates that downstream sediment composition is controlled by source lithology, hydraulic sorting, and sediment mixing. Weathering indices indicate increasing chemical alteration associated with longer sediment residence times in floodplain and channel bank deposits. These results show that downstream fining, increasing carbonate content, and vertical transitions from lithic-rich basal gravels to finer carbonate-rich overbank deposits record the combined effects of channel incision, sediment sorting, and river regulation.

Key words: Fluvial system, Sand composition, Channel evolution, Sedimentology, Depositional environment.

INTRODUCTION

Fluvial systems in the southern Alpine region of Europe are highly dynamic environments. The sedimentological and geomorphological characteristics of these landscapes are shaped by the complex interplay between tectonics and climate, hydrology, and sediment supply variability. The rivers of the southern Alps typically exhibit strong longitudinal gradients extending from steep mountain headwaters to low-gradient piedmont plains. These lead to pronounced downstream variations in grain size, sediment composition, and depositional processes (Garzanti *et al*., 2006) and reflect the combined influence of source lithology, physical and chemical weathering, and hydraulic sorting during transport (Folk, 1980; Jan and Eynatten, 2004; Garzanti *et al*., 2011). Extreme hydrological events and long-term channel adjustments, including incision and lateral migration, play a fundamental role in redistributing sediments and shaping fluvial landscapes in these environments (Surian *et al*., 2009, 2016; Comiti *et al*., 2011; Comiti, 2012; Ziliani and Surian, 2012; Scorpio and Piégay, 2021; Scorpio *et al*., 2024a; Brenna *et al*., 2026).

The last century has overseen substantial change in Alpine catchments. This can be attributed to both natural forcing and anthropogenic engineering, and includes channel narrowing, incision, and changes in channel pattern. Both transversal and longitudinal changes associated with gravel mining and anthropogenic land use changes have strongly modified sediment fluxes and impacted sediment connectivity and conveyance (Piton *et al*., 2016; Llena *et al*., 2019; Marchi *et al*., 2019; Cucchiaro *et al*., 2024; Piasecka *et al*., 2025; Pittau and Scorpio, 2026). These have been the focus of recent studies based on both historical cartogra-

[1] *Department of Geosciences, Eberhard Karls University of Tübingen, Schnarrenbergstraße 94-96, 72076 Tübingen, Germany.*
[2] *Department of Chemical and Geological Sciences, University of Modena and Reggio Emilia, via Campi 103, 41125 Modena, Italy.*
[3] *CNR-GEO, Corso Stati Uniti 4, 35127 Padova, Italy.*
[4] *School of Earth, Atmosphere and Environment, Monash University, 9 Rainforest Walk, Clayton VIC 3800, Australia.*
[*] *Corresponding author: Qutbudin Ishanch (qutbudin.ishanch@sedgeo.uni-tuebingen.de)*

phy and orthophoto analysis (Surian *et al.*, 2009; Comiti *et al.*, 2011; Ziliani and Surian, 2012; Scorpio *et al.*, 2018, 2020, 2024b).

Despite these advances, our understanding of the temporal and spatial changes in sediment characteristics in response to these documented geomorphological changes remains limited. Very few studies effectively integrate geomorphological with sedimentological approaches in order to investigate recent (Anthropocene) spatial and temporal evolution of Alpine fluvial systems. Nevertheless, a range of sedimentological tools have been shown to be effective for the reconstruction of sediment provenance, transport pathways, and depositional processes in Alpine contexts. These include grain-size analysis, sand petrography, and geochemical proxies (Garzanti *et al.*, 2006, 2011; Ravazzi *et al.*, 2012; Demurtas *et al.*, 2022, 2024); elemental geochemistry – particularly the use of immobile elements – to constrain sediment sources and mixing processes (McLennan, 1993); and weathering indices to inform chemical alteration, especially in mixed carbonate-siliciclastic systems (Garzanti, 2016). Given the degree of change observed, there is a clear need to integrate data from sedimentary processes across multiple depositional environments within fluvial systems such as channel beds, islands, floodplains, terraces, and channel banks with geomorphological investigations of change. However, the extent to which sedimentological characteristics record recent channel adjustment and anthropogenic modification in regulated Alpine rivers remains poorly understood.

We hypothesize that recent channel evolution – defined here as approximately the last 70 years – and anthropogenic modification will be reflected in measurable spatial and vertical variations in sedimentological characteristics. We propose that integrating sedimentological analyses with geomorphological reconstruction provides a more comprehensive understanding of sediment transport, storage, and channel adjustment than using these approaches independently.

This study investigates recent channel evolution in the Serio River, northern Italy, by integrating sedimentological and geomorphological approaches. The Serio River represents a highly dynamic Alpine river that has experienced substantial anthropogenic modification, including channel regulation, gravel extraction, and channel incision, making it an ideal case study for examining the relationships between sediment characteristics and channel evolution. By integrating grain-size distribution, sand lithology composition, major and trace element geochemistry, weathering indices, portable optically stimulated luminescence (pOSL), and geomorphological reconstruction, this study aims to:

(i) characterize downstream variations in sediment properties from mountain catchment to piedmont plain;
(ii) evaluate differences between channel bed and channel bank deposits, including changes through time preserved within bank stratigraphy;
(iii) assess sediment provenance and mixing processes using petrographic and geochemical tracers;
(iv) quantify weathering intensity and its relationship to sediment residence time and depositional environments; and
(v) examine the role of geomorphological dynamics and anthropogenic modifications in controlling sediment transport and storage.

This integrated approach provides new insights into how sedimentological characteristics record recent channel evolution and anthropogenic modification within a regulated Alpine river and demonstrates the value of combining sedimentological and geomorphological datasets to reconstruct recent fluvial adjustment.

STUDY AREA

The study focuses on the Serio River catchment on the southern side of the Alps in northern Italy (fig. 1). The Serio River forms part of the southern Alpine drainage network and is a major tributary of the Adda River within the Po River Basin.

The Serio River drains a catchment of approximately 1,256 km² over a length of 124 km in the Lombardy administrative region of northern Italy (Canobbio *et al.*, 2010). It rises in the Orobic Alps at about 3051 m a.s.l. and flows south-southwest through the Val Seriana before forming a broad Quaternary alluvial fan and ultimately joining the Adda River (fig. 1; Fontana *et al.*, 2014). The catchment represents a typical southern Alpine fluvial system, characterized by mixed carbonate-siliciclastic lithologies.

The catchment is characterized by a temperate alpine-pluvial climate regime with pronounced seasonality influenced by Atlantic weather systems and orographic precipitation patterns from the Mediterranean Sea (Isotta *et al.*, 2014). This regime yields relatively dry winters, wetter spring and autumn seasons, and warm summers with convective rainfall peaks (Cavalleri *et al.*, 2024). Mean annual precipitation decreases downslope from approximately 1500-2500 mm in the high alpine headwaters to around 800-1200 mm on the piedmont plain. Although snowfall contributes to seasonal snowfields above ~2000 m a.s.l., there are no significant contemporary glacier contributions to runoff in the catchment (Ménégoz *et al.*, 2020).

The basin exposes Southern Alpine basement rocks, including Variscan metavolcanics overlain by Permian-Triassic conglomerates and dolostones, as well as Triassic-Jurassic carbonates (fig. 1). These lithologies supply abundant carbonate lithic fragments, felsic volcanic material, chert, and amphibole-garnet-epidote heavy minerals,

together with piedmont plain quartz-feldspar inputs influenced by adjacent Oglio and Adamello sources (Ravazzi *et al.*, 2012).

Mountain catchment reaches are characterized by steep gradients and cobble-boulder channel beds, interrupted by several check-dams, water-withdrawal structures, and hydroelectric dams that fragment the channel, affect sediment conveyance, and locally reduce water availability. In the piedmont plain, the river shifts into a wider valley composed of gravel-cobble deposits, where urban-industrial effluents near Bergamo (fig. 1) and non-return irrigation withdrawals influence hydrological conditions. The main alluvial plain is dominated by braided gravel bars and seasonally drying pools during summer, receives treated wastewater discharge, and hosts intensive agriculture. Near Mozzanica (fig. 1), the channel evolves into a single-thread meandering pattern with mixed gravel-sand-silt deposits, reflecting its reduced gradient and increasing agricultural influence (Canobbio *et al.*, 2010; Viganò *et al.*, 2013; Albano *et al.*, 2017).

Official data (Regione Lombardia, 2024) indicate that approximately 40.000 m^3 (5715 m^3/y) of gravel was extracted from the channel in the mountain catchment from 1981 to 1987. Data on the alluvial plain area are not available, but orthophoto analysis (see section MATERIAL AND METHODS: Geomorphological analysis) shows evidence of gravel mining in both the active channel and the recent floodplain from 1954 through to the end of the 1980s. Po Basin Authority archives show that the active channel in the piedmont area was stabilized by bank protection works and levees built mainly between 1980s and 1990s.

MATERIALS AND METHODS

Field sampling and observations

Fieldwork focused on the collection of rock and sediment samples from different depositional settings along the Serio River and was conducted in February 2024.

Along the Serio River, sampling focused on both the mountain catchment and piedmont plain sectors, comprising 12 bedrock sampling sites and seven fluvial sediment sampling locations (from four study sites. fig. 2). Source rocks and channel bed surface sediments were collected from the mountain catchment; this sector is referred to hereafter as the upstream channel. On the piedmont plain – hereafter referred to as the downstream channel – samples were collected from channel beds, floodplains, islands, terraces, and four channel bank profiles, representing the principal depositional environments of the Serio River corridor. The bulk of the samples were collected from different geomorphological settings at four sites in the piedmont plain (fig. 2). Sediment samples were collected using a shovel by extracting the upper 5-10 cm of material from each sampling target. Sample locations and descriptions are provided in fig. 2 and table 1, while descriptions of the source rock samples are presented in Supplementary table S1.

The sampling strategy was designed to capture spatial variations in sedimentological characteristics across the mountain-to-piedmont transition and among contrasting depositional environments, thereby providing the basis for the integrated sedimentological and geomorphological analyses undertaken in this study.

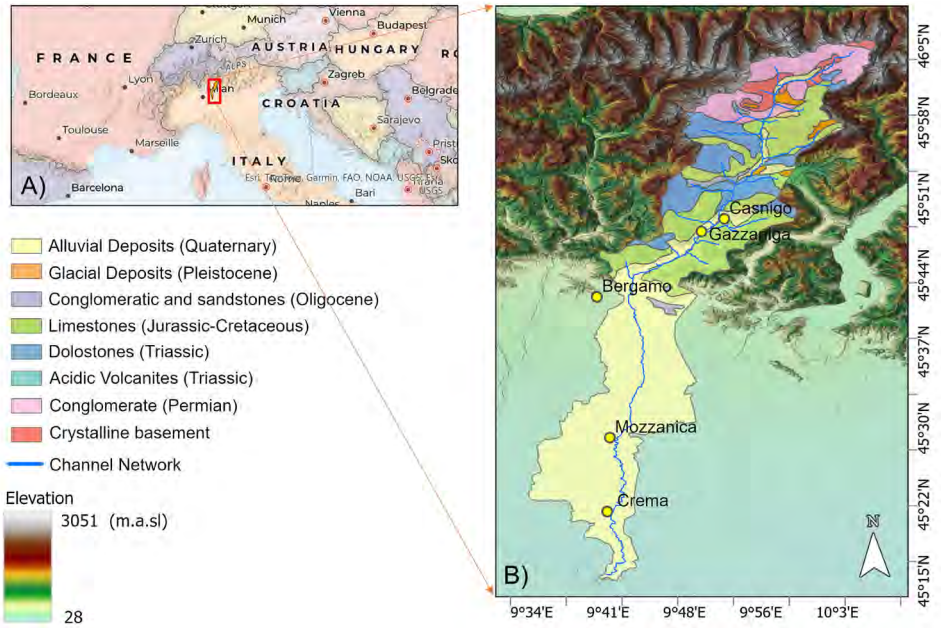


Figure 1 - Study area of the Serio River (A) and its geological setting and elevation (B).

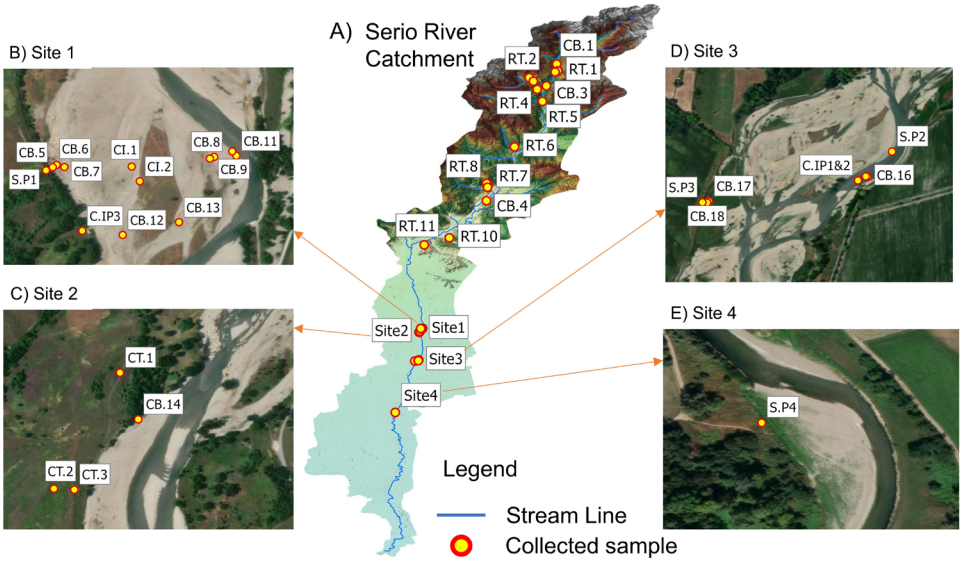


Figure 2 - Sampling locations in the Serio River catchment. (A) Overview of the Serio River catchment showing the location of all sampling Sites; (B) sampling locations at Site 1; (C) sampling locations at Site 2; (D) sampling locations at Site 3; (E) sampling location at Site 4.

Table 1 - Description of samples collected from the Serio River catchment, including sampling locations, corresponding sedimentary environments and facies.

Sample location	Sample ID	Sedimentary environment and facies	Longitude (°E)	Latitude (°N)	Elevation (m ASL)
Mountain Catchment	CB.1	Upstream channel bed	9.95	46.00	732
	CB.2		9.94	45.99	673
	CB.3		9.93	45.96	652
	CB.4	Sediment upstream from the Gazzaniga Dam	9.84	45.79	398
Piedmont plain (Site 1; fig. 2B)	CB.5	Sediment from the downstream channel bed	9.74	45.60	214
	CB.6		9.74	45.60	214
	CB.7		9.74	45.60	213
	CB.8		9.74	45.60	214
	CB.9		9.74	45.60	214
	CB.10		9.74	45.60	215
	CB.11		9.74	45.60	213
	CB.12		9.74	45.60	213
	CB.13		9.74	45.60	213
	C.IP3	Floodplain	9.74	45.60	214
	SP1	Channel bank profile	9.74	45.60	216
	CI.1	Island	9.74	45.60	215
	CI.2		9.74	45.60	214
Piedmont plain (Site 2; fig. 2C)	CB.14	Sediments from channel bed	9.74	45.59	210
	CT.1	Terrace	9.73	45.59	213
	CT.2		9.73	45.59	212
	CT.3		9.73	45.59	212
Piedmont plain (Site 3; fig. 2D)	CB.15	Sediments from downstream channel bed	9.73	45.55	180
	CB.16		9.73	45.55	180
	CB.17		9.73	45.55	178
	CB.18		9.73	45.55	178
	SP2	SP2 representing the left and SP3 the right-side channel bank deposits	9.73	45.55	183
	SP3		9.73	45.55	180
	C.IP1	Floodplain	9.73	45.55	180
	C.IP2		9.73	45.55	179
Piedmont plain (Site 4; fig. 2E)	SP4	Channel bank profile samples at Mozzanica town	9.70	45.47	140

Geomorphological Analysis

We undertook Geographic Information System (GIS) analyses using ArcGIS Desktop (ArcMap). Geological information was obtained from the Italian National Geoportal via an OGC Web Map Service (WMS) providing the Carta Geologica d'Italia (1:500,000 scale), which was integrated into the GIS environment. The resulting datasets were used to support the geological characterization and geomorphological interpretation of the study area (figs 1 and 2).

Geomorphological analysis of channel changes in terms of active channel width, channel pattern, and bed level was carried out for four representative reaches of the Serio River downstream channel. These sites represent longitudinal river sections ranging from 170 m at Site 1 to 450 m at Site 3. For each study site, the active channel was mapped for 18 time slices using topographic maps (1889), orthophotos (1954, 1975, 1980, 1988, 1997, 1999, 2002, 2003, 2007, 2012, 2015, 2018, 2021, and 2023), and satellite imagery (2019, 2020, and 2024). The average active channel width was estimated from regularly spaced transverse cross-sections positioned at approximately 50 m intervals along each study reach.

Bed-level changes from the 1950s to the present were estimated for each site using topographic cross-sections acquired in 2021 and/or 2024. Bed-level changes were evaluated as the differences in elevation between geomorphic surfaces (e.g., floodplains, bars, and the active channel) identified from the 1954 orthophotos, field observations, and the most recent imagery (2024). This procedure accounted for the potential presence and thickness of overbank deposits that accumulated where the former 1954 active channel had subsequently evolved into floodplains or terraces.

The geomorphological analyses provide the spatial and temporal context for interpreting sedimentological characteristics in relation to recent channel evolution.

Sedimentological analysis

Grain-size analyses for the fine-grained component (<2 mm) were undertaken on all samples using dynamic laser particle sizing. Bulk samples were oven-dried at 50 °C, gently disaggregated, and homogenized prior to conducting grain size measurement. The material was then sieved to separate the <2 mm fraction (hereafter referred to as the fine-grained fraction) for grain-size analysis. Grain-size distribution and grain shape were determined using a Microtrac Sync Particle Analyzer (Microtrac Retsch GmbH, 2023). This method offers several advantages over traditional techniques, including minimal sample preparation and rapid measurement (Wang *et al.*, 2017; Schulte *et al.*, 2018). We undertook end-member modeling of the resulting data using the Python-based QGrain app (Liu *et al.*, 2021) to identify grain populations and relate them to likely transport processes and depositional environments.

In addition to laser particle-size analysis of the <2 mm fraction, we analyzed the size distribution of coarse-grained surface sediments (>2 mm) using both quantitative and qualitative approaches. At Site 1, a representative river cross-section was surveyed using a drone, and images extracted from the recorded video were analyzed using ImageJ (Schneider *et al.*, 2012). Each image represented an area of approximately 2×2 m, from which approximately 500 coarse particles (>2 mm) were randomly measured to calculate the median grain size (D50) and quantify lateral grain-size variability across the cross-section. Field photographs of the channel bed and the corresponding channel-bank profile were used to visually compare present-day coarse channel-bed sediments with the coarse basal deposits exposed in the channel bank, and to qualitatively assess the relationship between surface sediment characteristics and preserved channel-bank stratigraphy (fig. 4A-D).

We analyzed the lithologies of the sand-sized fractions of all samples. For grain lithological analysis, the sand fraction (0.063-2.00 mm) of each sample was isolated and split. A small portion was embedded in Araldite to produce blocks from which thin sections were prepared. The thin sections were stained with Alizarin Red solution to distinguish calcite from dolomite grains. Petrographic modal analysis was performed using an optical microscope by counting at least 300 grains per sample with a grid spacing of 0.5 mm (or 1 mm for moderately sorted samples). The analysis followed the Gazzi-Dickinson method (Ingersoll *et al.*, 1984) to minimize grain-size dependence on composition, whereby we continued counting until at least 300 lithic fragments were identified. The results are summarized in table 2 and plotted in ternary diagrams (fig. 5) and compared with available reference databases (Garzanti *et al.*, 2006).

We undertook portable optically stimulated luminescence (pOSL) analyses of the bulk sediment from the channel bank profile samples with the aim of gaining an insight into relative ages with depth (Sanderson and Murphy, 2010). Portable OSL provides a rapid overview of the relative age of bulk sediment samples, based on the assumption that older deposits will produce stronger luminescence signals (Sanderson and Murphy, 2010). Signal variations down a profile may also reflect differences in mineral composition and environmental radiation dose-rate. In this study, we conducted pOSL measurements on samples from four channel bank profiles (SP1-SP4) along the Serio River and compared the resulting signals with lithological and geochemical compositions to identify potential event-based depositional phases.

Geochemical Data

Major, minor, and trace element concentrations were determined using X-ray fluorescence (XRF) spectrometry and measured in the Department of Geology, Johannes Gutenberg University of Mainz, Germany. Sample preparation and analytical procedures followed standard methods (Govindaraju, 1989). All samples, including source rocks, were powdered using a binder mixture to obtain a grain size of <63 μm. Approximately 2 g of fine powder was prepared for major element analysis, while an additional 6 g was used for trace element measurements.

We used the geochemical results to assess chemical weathering using both the Al_2O_3/CaO (AC) ratio and Weathering Index for Carbonates (WIC). The Al_2O_3/CaO ratio serves as a proxy for weathering intensity and lithological mixing, since Al is largely immobile and associated with aluminosilicate phases, whereas Ca is predominantly hosted in easily weathered carbonate minerals (Nesbitt and Young, 1982; McLennan, 1993). Higher AC ratios therefore indicate increased weathering or a greater siliciclastic contribution, whereas lower values reflect stronger carbonate influence. In carbonate-rich Alpine catchments, CaO variability is often controlled by lithology rather than by weathering alone, which can bias conventional indices such as the Chemical Index of Alteration (CIA). To overcome this limitation, we also used the Weathering Index for Carbonates (WIC; Eq. 1), since it accounts for carbonate dilution effects and provides a more reliable assessment of weathering in mixed carbonate-siliciclastic systems (Garzanti, 2016). The combined use of these proxies allows for a more robust evaluation of weathering processes and sediment sources in both catchments.

$$WIC(\%) = \frac{Al_2O_3}{Al_2O_3 + CaO + MgO} \times 100 \qquad \text{Eq. 1}$$

RESULTS

The Serio river exhibits a heterogeneous composition, combining siliciclastic and carbonate components across all depositional environments, including mountain catchment and piedmont plain settings. We observe variations in grain size, lithology, and geochemical composition along the channel section profile and between different geomorphic settings.

Recent geomorphological evolution of the Serio River fluvial corridor.

Geomorphological analysis reveals considerable channel morphological dynamics since the end of the 19th century at the Serio River sites analyzed. Specifically, the active channel reached its maximum width in 1889, with average values of 700 m at Site 1, 900 m at Site 2, 850 m at Site 3, and 500 m at Site 4 (fig. 3A). Subsequently, the active channel experienced significant narrowing at all study sites until 1988, when channel widths decreased to 131 m at Site 1, 115 m at Site 2, 140 m at Site 3, and 45 m at Site 4 (fig. 3A). From the early 1990s onwards, channel width trajectories were characterized by alternating phases of narrowing and widening (fig. 3A). In 1997, channel widths were 145 m at Site 1, 115 m at Site 2, 250 m at Site 3, and 57 m at Site 4, while in 2024 they reached 260 m at Site 1, 150 m at Site 2, 290 m at Site 3, and 65 m at Site 4 (fig. 3A).

Over the same period, and especially after the 1950s, the riverbed experienced widespread vertical incision, amounting to approximately 2.5 m at Site 1, 4 m at Site 2, and 3 m at Sites 3 and 4. The measured incision occurred between 1954 and 2024 (fig. 3B), with the highest rates recorded between the 1970s and 1990s.

Despite these substantial morphological changes in terms of channel width and bed level, channel planform patterns remained stable at Sites 1 (figs 3C-H) and 4 throughout the entire study period, maintaining braided and meandering morphologies, respectively. By contrast, Sites 2 and 3 exhibited a braided morphology from 1889 to 1976, followed by a transition to a wandering pattern between 1988 and 2000; after the early 2000s, a braided pattern again became predominant.

At all sites, the result of the combined effects of bed incision (from 2.5 to 4 m) and channel narrowing caused the suspension of a sector of the former channel – active until the 1950s-1970s – and led to the formation of recent terrace surfaces located approximately 3-4 m above the present active channel. Subsequently, channel dynamics were mainly driven by lateral migration of the active channel through bank erosion processes, which produced the alternating phases of narrowing and widening observed after the early 2000s.

Sites from 1 to 3 present a braided or wandering pattern over the last decades, characterized by the diffusive islands colonized by pioneer vegetation. Islands show temporal variability in their extent, shape, and position across different years (figs 3F-H).

Analyses indicate that island formation and erosion, but even bank erosion, channel widening primarily occurred during major flood events, particularly those of 26 November 2002, 30 October 2013, and 28 October 2018 (ARPA Lombardia, 2025).

Grain Size

Fine grain-size characteristics (<2 mm) of the Serio River sediments indicate very poorly to poorly sorted material, yielding ϕ values (Folk, 1980) exceeding 1. Mean grain sizes range from 148 μm in the mountain catchment samples to 16 μm in channel bank profile deposits, with modal val-

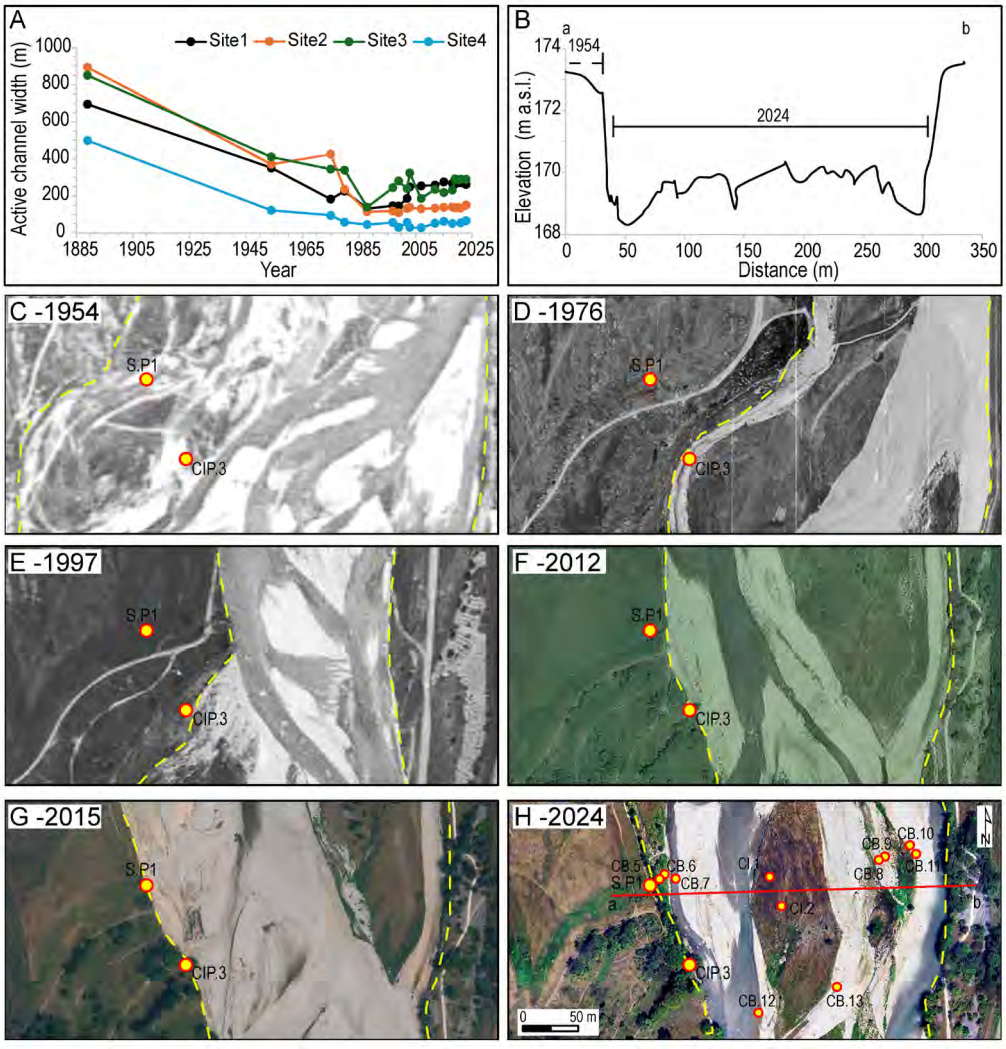


Figure 3 - A. Channel width evolutionary trajectory from 1889 to 2024 at the four studied sites of the Serio River. B. Topographic cross-sections showing channel incision at Site 1 between 1954 and 2024 (for location of the cross-section see fig. 3H). C-H. Orthophotos, samples location and active channels mapped in (C) 1954; (D) 1976; (E) 1997; (F) 2012; (G) 2015; (H) 2024.

ues between 543 µm and 5 µm. Skewness is predominantly fine-skewed across all samples, whereas surface channel bank deposits display near-symmetrical distributions (Figs S1–S6; table S2).

In the mountain catchment, grain-size distributions show that the largest dominant grain size occurs in sample CB.1 (322 µm), while the smallest is observed in CB.2 (10 µm). The greatest variability is recorded in CB.3, ranging from approximately 11 µm to 645 µm, whereas CB.4 exhibits the lowest variability, with grain sizes between 18 µm and 161 µm (fig. S1).

On the piedmont plain, downstream channel bed sediments (fig. S2) show distinct grain-size distributions. Sample CB.9 (fig. S2a) exhibits a modal grain size of 4 µm, representing 13.85% of the analyzed distribution, while samples CB.7, CB.11 (fig. S2b), and CB.17 (fig. S2c) are characterized by a modal grain size of 322 µm, reaching up to 35% of the grain-size distribution. Island deposits (fig. S3) are dominated by a modal population of approximately 14 µm, representing about 60% of the distribution in sample CI.1. Floodplain sediments (fig. S4) exhibit a range of modal grain sizes from 2 µm in sample C.IP.1 to 322 µm in sample C.IP.2. Terrace deposits (fig. S5) are characterized by modal grain sizes ranging from 14 µm to 47 µm.

Grain-size distributions within the channel bank profiles are generally fine upwards. In profile SP1 (fig. S6a), the modal grain size increases progressively from approximately 1 µm (9% of the distribution) in the surface sample (SP1.1) to 229 µm (23%) in the basal sample (SP1.5). In profile SP2 (fig. S6b), the upper samples are dominated by very fine sands (74-105 µm), coarsening downwards to coarse sands (590 µm) in SP2.3. In profile SP3 (fig. S6c), the upper samples are characterized by fine silts (9-16 µm) and coarsen downwards to fine sands (mode of 209 µm) in SP3.6. Similarly, profile SP4 fines upwards from medium sands (384 µm) at the base (fig. S6d).

The coarse-fraction (>2 mm) distribution at Site 1 exhibits pronounced lateral variability across the river cross-section (fig. 4D). Median grain size (D50) is lowest

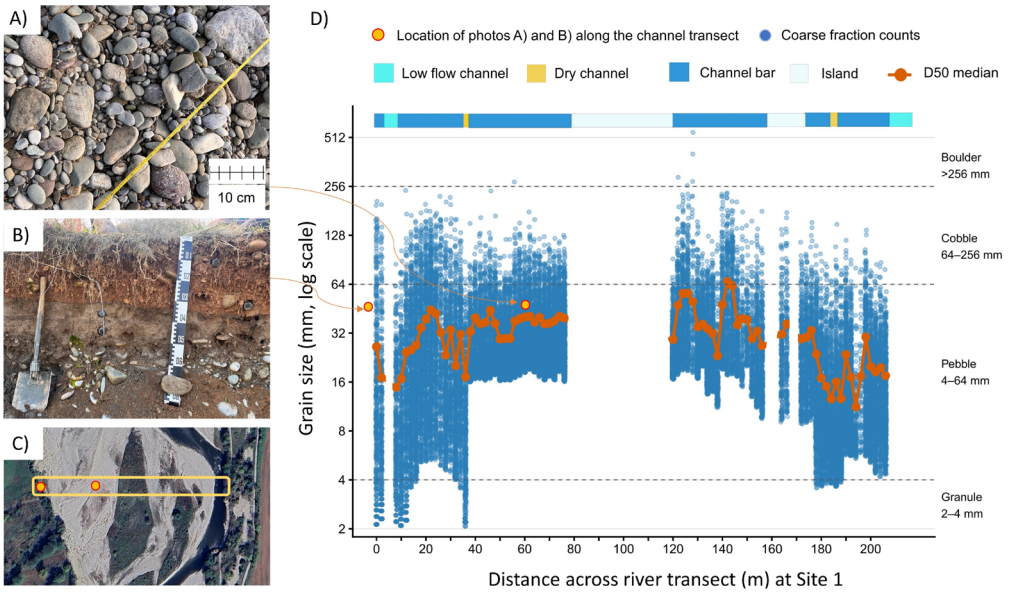


Figure 4 - Coarse sediment characteristics and spatial grain-size distribution across the channel transect at Site 1. (A) Unmanned Aerial Vehicle (UAV) derived aerial image showing the surveyed transect used for coarse-fraction analysis, with a 10 cm scale bar. (B) Channel bank profile adjacent to the transect, illustrating the stratigraphy of recent fluvial deposits. (C) Aerial photo of the selected transect site. (D) Spatial distribution of ImageJ-derived coarse grain sizes (>2 mm) measured at 2 m intervals along the transect. The colored bar above the plot indicates the geomorphic units along the transect. White (no data) sections indicate locations where the presence of water or dense vegetation in the low-flow channel or on vegetated islands prevented grain-size measurements.

in lateral low-flow and dry channels, ranging from approximately 14 to 20 mm, and increases on channel bars, where D50 commonly ranges between 32 and 64 mm, and the margins of vegetated islands, where D50 is around 40 mm. Individual coarse particles reach a maximum size of approximately 512 mm, with the largest clasts concentrated on channel bars and island margins. The corresponding channel-bank profile exposes a distinct basal coarse gravel layer (fig. 4B), consisting of a heterogeneous sandy-gravelly deposit dominated by pebbles with scattered cobbles. A comparable grain-size distribution is observed across the modern channel-bed surface, where pebble-sized particles dominate most of the transect, accompanied by locally abundant cobbles and occasional isolated boulders.

Bulk sand composition

Channel surface deposit lithologies. Thin section analyses of the Serio River sand samples are summarized in table 2. Samples are dominated by lithic rock fragments (r.f.), with a generally low abundance of quartz (ca <15%) and only rare occurrences of feldspar (~1%) (fig. 5). The lithic grain composition shows an approximately equal contribution of carbonate (CE) and non-carbonate (L) fragments (fig. 5). The major lithological composition of sediments along the channel across different geomorphological features is illustrated in fig. S7.

Channel bed deposits from the upper mountain catchment (CB.1, CB.2, and CB.3) plot predominantly toward the non-carbonate lithic vertex, with carbonate contents not exceeding ~30% and crystalline sand fractions exceeding 60% (fig. 5). These samples contain notable proportions of metamorphic and volcanic rock fragments. The lower mountain catchment sample (CB.4) shows an increase in carbonate fraction, since it is located further downstream with greater potential for carbonate rocks to contribute to the river sediments (fig. 1). Channel bed deposits from piedmont plain river bars yield abundant crystalline lithic fragments exceeding >30% (fig. 5). By contrast, the overbank and terrace deposits are more carbonate-rich (>60%) and dominated by dolostone. Island and floodplain sediments also yield carbonate contents exceeding 50% (fig. 5).

Downstream, on the piedmont plain, we observe a relative decrease in sandstone and carbonate components and an increase in siliciclastic fragments (Samples CB.5-11 from the Site 1 transect; table 2 and fig. S7). Sample CB.12, located at the tail of the island, yielded a higher dolostone content. The most downstream channel bed sample (CB.18) is characterized by relatively higher proportions of non-carbonate lithic fragments.

Overbank deposits on the piedmont plain yield variable compositions. The terrace sample CT.3 shows the highest abundance of dolostone, floodplain sample C.IP.1 shows the highest limestone content, and terrace sample CT.2 contains the highest proportion of sandstone (table 2 and fig. S7).

Channel profile section lithologies. The four channel bank profiles investigated in this study (at Sites 1 through 4) yield variable lithologic compositions down their stratigraphy. The uppermost layers relate to overbank facies, while the lower units represent earlier channel bars (figs 5 and 6, table 2).

Three stratigraphic units are exposed at profile SP1 at Site 1 (fig. 6A). The uppermost 30 cm (two samples) is dominated by siliciclastic siltstone and sandstone, with minor

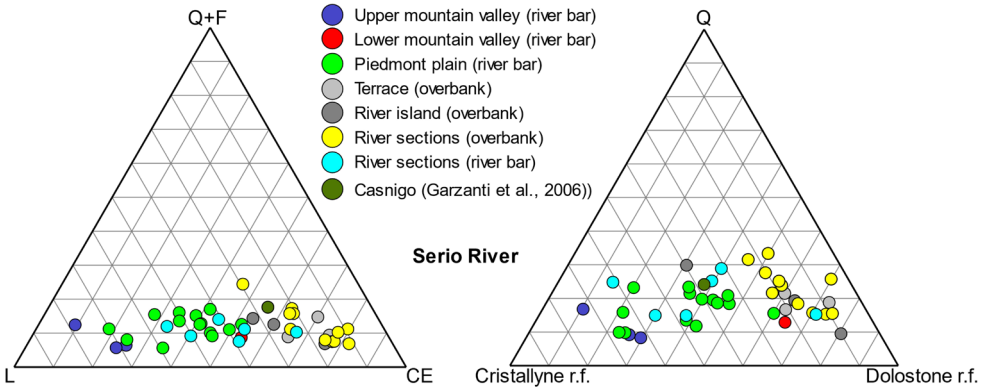


Figure 5 - Lithological composition of the Serio River across different geomorphological settings, including samples from Casnigo, located near Gazzaniga (see fig. 2A). Q+F denotes quartz and feldspar; L indicates lithic fragments; CE refers to carbonate rock fragments; crystalline r.f. denotes crystalline rock fragments; dolostone r.f. indicates dolostone fragments; and volcanic r.f. represents volcanic rock fragments.

dolostone and limestone, and rare volcanic, metamorphic and chert clasts. The underlying unit is more grey in color and is dominated by dolostone, then limestone, with siltstone and sandstone only a minor component. The lowermost unit, beginning at c. 50 cm depth, is a poorly sorted mix of cobbles and finer material but with a similar composition.

We observed four stratigraphic units in profile SP2 at Site 3 (fig. 6B), with variable clast composition (fig. 6B and table 2). The uppermost unit (sample SP2.1) is dominated by dolostone, with subordinate limestone and minor other lithologies. This unit is underlain by a layer dominated by limestone, with reduced dolostone and increased proportions of metamorphic and volcanic clasts (Sample SP2.2), below which is another unit (Sample SP2.3) characterized by low carbonate content, abundant metamorphic and volcanic clasts, moderate dolostone, and minor siltstone/sandstone and plutonic/gneissic components. The lowermost unit is compositionally mixed and dominated by volcanic clasts, with subordinate limestone and metamorphic components.

Profile SP3 is located 500 m downstream of the preceding two profiles, comprises three stratigraphic units, and likewise yields variability in clast composition (fig. 6C and table 2). The uppermost unit is dominated by siltstone/sandstone, with subordinate dolostone and minor limestone rock fragments, and rare metamorphic and volcanic clasts. The uppermost part of the middle unit has a similar composition, which grades into a more dolostone-rich composition and higher proportions of limestone, metamorphic, and volcanic clasts. The lower part of the middle unit comprises a higher limestone component, some metamorphic and volcanic clasts, and lower siltstone/sandstone. The lowermost unit (Sample SP3.6) hosts high proportions of metamorphic and volcanic clasts, moderate dolostone and limestone, and minor sandstone, plutonic/gneissic and chert components.

Only two samples were collected from SP4, which comprises a finer-grained upper and coarser, more cobble rich lower unit (fig. 6D and table 2). The upper unit (Sample SP4.1) is dominated by dolostone and limestone, with subordinate siltstone/sandstone and minor volcanic, metamorphic, and chert clasts, and overlies a more lithic-rich unit (Sample SP4.2) dominated by metamorphic and volcanic clasts, with subordinate limestone and minor chert.

Elemental geochemistry and weathering indices

The major element concentrations, obtained from XRF analyses, are summarized in table 3, with detailed values for all samples provided in Supplementary table S3. The mountain catchment channel bed sediments are dominated by SiO_2 (approximately 54 wt%), compared with lower concentrations on the piedmont plain (channel bed, floodplain, island, and terrace deposits: ~35 and 40 wt%). The next most prevalent element, Al_2O_3, is also highest in the mountain catchment channel bed samples (15 wt%). By contrast, MgO and CaO concentrations are higher on the piedmont plain, yielding ~7 wt% (island samples) and ~5 to 18-20 wt% (channel bed, floodplain, island, and terrace deposits) respectively. The least prevalent major element, K_2O, yields its highest concentrations (~4 wt%) in the upper valley channel bed samples (table 3).

The Site 1 transect on the piedmont plain provides an opportunity to investigate the distribution of major elements across a number of depositional contexts. We observe a range in SiO_2 concentrations from 33% to 41%, with the highest concentration in channel bed sample CB.7, and lowest concentration in island sample CI.2. CaO concentrations range between ~17% and 21% along the transect, with relatively higher values observed in channel bed samples. MgO varies from ~3.5% in CB.7 to ~7.5% in CI.2, with elevated values in island deposits. Al_2O_3 concentrations (~8-9%) and K_2O (~1.8-2%) show limited variability across all depositional settings, while Fe_2O_3 concentrations range between ~2.8% and 3.2% (fig. S8; table S3).

Table 2 - Summary of major sand lithological composition in the Serio River samples, based on thin-section analysis. Sandstone (%) includes carbonate and siliciclastic siltstone fragments. Quartz (Q) and feldspar (F) represent contributions from various sources, including volcanic, metamorphic, plutonic, and sedimentary rocks, as well as single grains and replacement phases.

Serio River sand major composition									
Sample location	Sample ID	Sandstone %	Dolostone %	limestones %	plutonic/gneissic rocks %	Metamorphic rocks %	Volcanic rocks %	Quartz + Feldspar	chert %
Upper mountain valley	CB.1	7.7	19.1	2.7	3.4	38.6	27.6	5.7	0.0
	CB.2	5.7	6.0	2.3	10.6	37.9	36.2	12.3	0.3
	CB.3	3.5	17.1	6.6	12.2	34.1	24.7	6.3	0.0
Lower mountain valley	CB.4	1.3	35.0	16.2	1.0	13.2	29.2	8.6	0.6
Piedmont plain	CB.5	13.2	24.4	14.9	4.3	21.6	16.5	12.2	0.3
	CB.6	0.7	31.0	9.2	1.1	28.2	26.4	12.4	0.3
	CB.7	5.5	29.7	6.5	8.0	23.6	21.4	16.7	0.3
	CB.8	5.0	25.9	4.0	5.4	27.1	27.5	15.9	2.3
	CB.9	1.6	26.3	11.4	3.6	23.2	28.2	12.3	0.6
	CB.10	3.0	21.6	16.3	1.0	32.0	20.0	12.0	0.6
	CB.11	0.0	21.6	16.3	0.7	35.2	22.8	15.0	0.6
	CB.12	6.5	37.7	4.9	0.0	17.3	29.0	11.0	0.3
	CB.13	4.7	15.0	0.6	9.3	34.1	27.7	7.8	7.8
	CB.14	1.3	11.0	16.5	6.6	29.6	30.7	15.5	0.6
	CB.15	2.0	25.0	16.0	6.3	23.0	13.0	9.9	1.0
	CB.16	4.7	27.5	12.1	6.3	30.5	14.1	9.1	0.0
	CB.17	12.4	13.0	12.1	2.9	38.1	19.7	5.9	0.3
	CB.18	4.0	13.3	1.3	8.4	36.4	30.1	10.7	5.3
Floodplain	C.IP.1	4.5	8.3	33.8	0.0	21.7	16.6	14.4	0.6
	C.IP.2	7.5	46.5	19.5	0.0	5.7	12.6	6.9	1.3
	C.IP.3	5.4	32.0	29.6	1.8	11.0	16.7	17.0	0.7
Island	CI.1	10.7	36.2	13.3	1.4	10.6	21.6	12.3	0.3
	CI.2	3.0	40.0	20.0	1.0	8.0	15.0	10.0	1.0
Terrace	CT.1	5.4	32.0	29.6	1.8	11.0	16.7	8.8	0.7
	CT.2	38.9	24.6	14.0	0.0	9.7	4.5	9.3	0.3
	CT.3	10.5	49.5	7.3	0.0	7.9	10.5	14.1	2.2
bank profile at site 1 (overbank-river section)	SP1.1	56.0	10.0	11.0	0.0	6.0	7.0	16.6	1.0
	SP1.2	50.0	11.0	12.0	0.0	7.0	8.0	11.7	0.5
	SP1.3	20.6	29.1	30.9	0.6	4.8	4.8	6.8	0.6
	SP1.4	9.4	35.6	26.8	0.0	4.7	16.8	7.9	0.7
	SP1.5	3.9	33.1	26.4	1.1	8.4	15.7	10.3	3.4
Channel bank profile at site 3 (overbank-river section)	SP2.1	8.7	30.7	23.6	0.0	4.7	15.7	11.1	3.1
	SP2.2	8.0	11.5	42.0	0.0	21.8	12.6	11.2	0.0
	SP2.3	3.8	29.2	3.8	2.5	29.8	25.1	7.6	0.0
	SP2.4	5.0	18.0	23.3	0.7	13.7	30.0	14.0	0.3
Channel bank profile at site 3 (overbank-river section)	SP3.1	37.4	21.5	4.3	0.0	11.3	9.3	16.6	0.3
	SP3.2	43.4	30.7	4.2	0.0	1.9	7.8	16.6	0.0
	SP3.3	23.1	28.0	13.3	0.0	12.1	11.7	11.7	0.0
	SP3.4	6.5	31.3	22.9	0.0	10.3	13.2	14.8	1.0
	SP3.5	1.4	32.8	11.1	0.0	12.8	17.9	15.5	0.0
	SP3.6	9.7	14.1	16.1	2.4	25.0	22.6	24.3	1.2
Channel bank profile at site 4 (overbank-river section)	SP4.1	8.7	42.2	23.6	0.0	5.0	8.7	8.9	0.0
	SP4.2	16.1	6.5	19.6	1.2	30.4	21.4	9.0	1.2

Table 3 - Summary of major and trace element concentrations in the Serio River.

Elements			Serio River									
	RMS rel*	Mountain catchment (n**=4)	Piedmont plain (n=6)	Island (n=2)	Flood Plain (n=3)	Terrace (n=3)	Channel bank profiles SP1 (n=5)	SP2 (n=4)	SP3 (n=6)	SP4 (n=2)		
			Composition % ±SD									
Major elements	SiO_2	g/100g	0.6	54±13	39±3	36±3	37±2	36±1	43±12	35±2	42±2	38±5
	Al_2O_3		0.7	15±4	9±0	9±1	8±1	8±1	12±6	6±1	11±2	8±1
	Fe_2O_3		0.5	5±1	3±0	3±0	3±1	4±1	5±2	2±1	4±1	3±0
	MgO		0.5	3±2	5±1	7±2	5±2	4±1	4±2	3±1	5±0	5±3
	CaO		0.7	6±9	19±1	18±2	20±3	16±3	13±12	26±3	15±3	20±2
	K_2O		0.6	4±1	2±0	2±0	2±0	1±0	2±1	1±0	2±0	2±0
	LIO		0.6	10±10	23±2	25±1	24±2	29±3	20±8	25±1	21±1	23±3
Trace elements	Sc	µg/g	8.4	15±2	12±1	11±0	12±0	12±1	16±5	12±1	14±2	11±2
	Cr		3.7	55±4	57±11	59±5	56±15	129±37	83±23	48±17	56±9	56±2
	Zn		2.4	185±183	424±175	446±83	995±607	6282±2328	3087±3109	1793±2214	114±74	954±79
	Ga		4.0	19±6	10±1	9±0	7±1	0±0	9±12	4±3	13±2	7±1
	Rb		1.5	185±58	89±5	85±8	79±10	66±8	107±55	62±8	101±13	79±6
	Sr		1.6	120±56	209±17	184±28	231±79	158±26	167±121	327±67	169±23	222±73
	Zr		1.7	163±33	121±7	127±2	122±18	169±45	140±35	98±24	133±22	124±15
	Cs		7.2	29±6	12±1	10±4	12±2	10±1	13±6	9±1	14±4	13±3
	Ba		2.6	489±132	280±14	289±28	288±63	360±90	453±156	207±79	304±61	272±75
	Pb		2.7	40±33	70±30	73±10	170±105	1094±446	520±545	327±372	51±48	209±54
	Th		6.6	13±3	8±1	7±1	7±1	9±2	9±4	6±1	9±1	7±2

* RMSrel: relative Root Mean Square error; n**: number of samples.

Major oxide concentrations vary systematically with depth and correspond to the stratigraphic units identified in the lithological description (figs 5 and 6; table 2).

Unit 1 is characterized across all profiles by relatively higher concentrations of silicate-associated oxides, although the magnitude of enrichment varies laterally. At SP1 (fig. 6A), on the western bank of Site 1, Unit 1 shows high SiO_2 (~55 wt%) and Al_2O_3 (~20 wt%), with low CaO (~1 wt%). K_2O concentrations decrease with depth, and SiO_2 and Al_2O_3 decrease progressively toward the base of the profile. Fe_2O_3 increases from the surface to the Unit 1-2 transition (~10-30 cm). In contrast, Unit 1 at SP2 (fig. 6B) shows more uniform compositions, with SiO_2 (~32-37 wt%) and Al_2O_3 (~5-8 wt%) remaining relatively constant down-profile. At SP3 (fig. 6C), Unit 1 exhibits higher Al_2O_3 (~12 wt%), K_2O (~4.8 wt%), and Fe_2O_3 (~2.3 wt%) relative to underlying units. At SP4 (fig. 6D), Unit 1 is comparatively more carbonate-influenced, with CaO (~19 wt%) and SiO_2 (~32 wt%), and higher Al_2O_3, MgO, K_2O, and Fe_2O_3 relative to the underlying unit.

Unit 2 represents a transitional interval across all profiles, marked by decreasing silicate oxides and increasing carbonate-associated components. In SP1 (fig. 6A), this transition occurs below ~30 cm, where CaO increases sharply and MgO rises from ~1.5 wt% to higher values, while SiO_2 and Al_2O_3 decrease. In SP2 (fig. 6B), CaO increases from ~21 wt% at the surface to ~30 wt% at ~160 cm depth, while Fe_2O_3, K_2O, and MgO decrease downward through this unit. SP3 (fig. 6C) shows a more variable trend, with fluctuating SiO_2, decreasing Al_2O_3 (~12 to ~8 wt%), K_2O (~4.8 to ~3 wt%), and Fe_2O_3 (~2.3 to ~1.9 wt%), accompanied by increasing CaO (~10 to ~18 wt%). At SP4 (fig. 6D), Unit 2 is characterized by increasing SiO_2 (~32 to ~42 wt%) and CaO (~19 to ~22 wt%), and decreasing Al_2O_3, MgO, K_2O, and Fe_2O_3.

Unit 3 is consistently carbonate-dominated across all profiles, although it shows variable detrital input. In SP1 (fig. 6A), CaO reaches a maximum of ~25 wt% toward the base of the profile (~70 cm), while MgO increases to ~5 wt% and silicate oxides decrease. In SP2 (fig. 6B), Unit 3 is associated with peak CaO concentrations (~30 wt% at ~160 cm), followed by a decrease toward the base, while Fe_2O_3, K_2O, and MgO increase again below this level. In SP3 (fig. 6C), Unit 3 is moderately carbonate-influenced, with elevated CaO (~18 wt%) and continued relatively high silicate and lithic contributions compared to other profiles. In SP4 (fig. 6D), this unit is characterized by increased CaO (~22 wt%) and reduced silicate oxide concentrations.

Unit 4 is only clearly developed in SP1 and SP2 and represents a heterogeneous basal interval. In SP1 (fig. 5A), this unit corresponds to the lowermost part of the profile (~70 cm), where CaO remains elevated and silicate oxides

are reduced. In SP2 (fig. 6B), Unit 4 occurs below ~160 cm and is marked by decreasing CaO and increasing Fe_2O_3, K_2O, and MgO, indicating increased compositional variability. In SP3 (fig. 6C) and SP4 (fig. 6D), a distinct Unit 4 is not observed, and instead a gradual transition into heterogeneous basal compositions is present.

The results of the weathering index calculations are presented in fig. 7. We observe consistently low values for both the WIC and the AC ratio irrespective of location within the catchment.

In the channel bank profile at Site SP1, both indices increase markedly toward the surface, with WIC values reaching up to ~83% and AC ratios up to ~25, indicating very high weathering intensity in the upper layers. In contrast, the lower part of the SP1 profile shows lower values, corresponding to weaker weathering.

At Site SP3, weathering indices show a decrease from moderate values in the upper layers to lower values toward the base of the profile (fig. 7) with detailed variations in these trends shown in Supplementary fig. S9.

Portable OSL (pOSL) analyses of the profile samples

We undertook pOSL measurements of luminescence signal in the bulk sediment for the two profiles containing suitably fine-grained material (SP1 and SP3) to investigate relative changes in signal, and presumably age, down those profiles (fig. 6). Overall, the down-profile trends in both blue (proxy for quartz) and infrared (proxy for feldspar) signals are consistent within individual profiles.

The profile SP1 yields an unexpected down-profile trend, however: signals increase in intensity for the up-

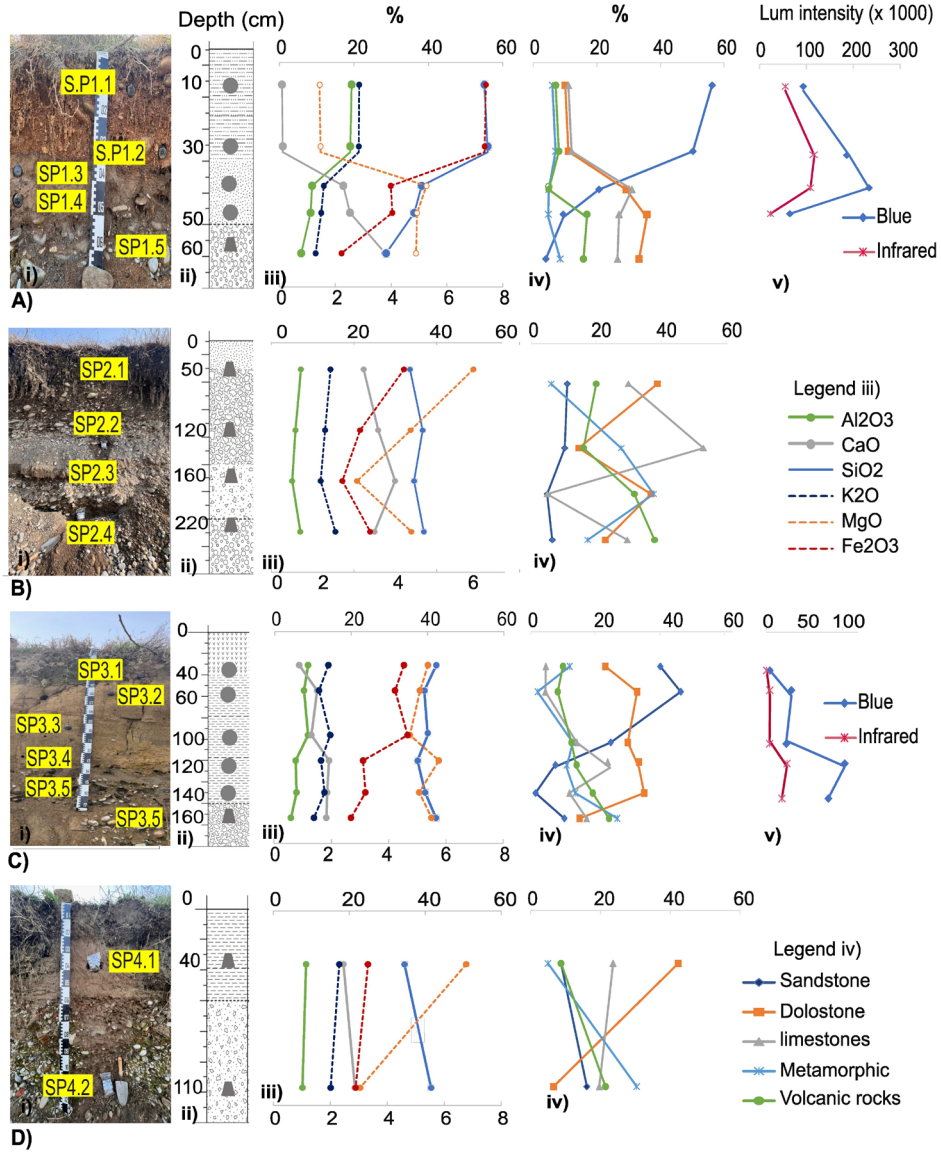


Figure 6 - Channel bank profiles of the Serio River at Sites 1-4. A.i) Field photographs of the profiles; A-ii) stratigraphic logs; A-iii) major element concentrations for selected samples, where the upper horizontal axis corresponds to Al_2O_3, CaO, and SiO_2, and the lower axis corresponds to K_2O, MgO, and Fe_2O_3; A-iv) sand lithology composition; and A-v) pOSL intensity counts. Figures A-D corresponds to Site 1 (SP1), Site 2 (SP2), Site 3 (SP3), and Site 4 (SP4), respectively.

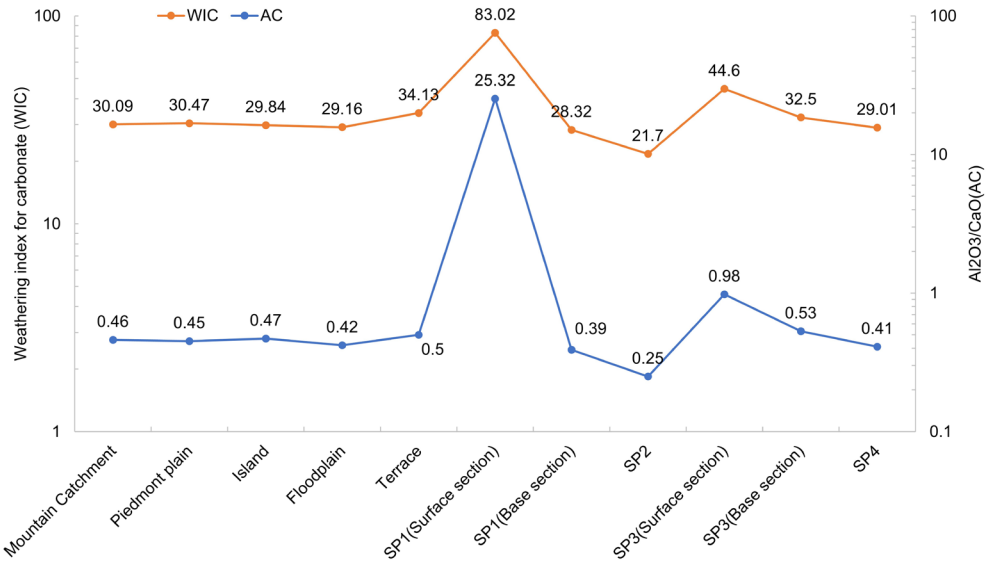


Figure 7 - Weathering index of Serio river sediment deposits along the channel bed and overbank.

permost three samples, then decrease for the lowermost sample at 50 cm depth. This trend suggests either an age inversion in the lowermost sample, or a decrease in environmental dose rates for that sample leading to a lower overall dose received. The latter is possible given the increase in low-radiation dolostones and limestones present at that lower depth. (fig. 6A-v).

Luminescence intensities increase down-profile within profile SP3, with a substantial increase in the blue signal at c. 120 cm depth consistent with a stratigraphic contact between fine and coarser grained sediments. We infer this change to suggest an increase in depositional age associated with that stratigraphic break (fig. 6C-v).

Provenance tracers

Trace-element concentrations for both catchments are summarized in table 3, with detailed values provided in Supplementary table S4. Provenance relationships based on Sc-Zr-Th systematics are illustrated in fig. 8. Source rock samples define distinct compositional fields: RT1 (metavolcanic rock) is enriched in Zr (~50%), RT3 (Permian conglomerate) shows higher Sc values (~56%), and limestone samples (RT9 and RT11) plot toward the Sc-rich domain, reaching up to ~70%.

In the Serio River, upstream channel bed sediments from the mountain catchment plot toward higher Th proportions (up to ~30%), whereas piedmont plain samples show reduced Th (~20%) and relatively higher Sc contributions (up to ~40%). Channel bank profiles display variable compositions indicating change through time: SP1 samples are characterized by elevated Sc values (up to ~45%) and moderate Th (~28%), while SP2 samples show comparatively lower Th values (~18%).

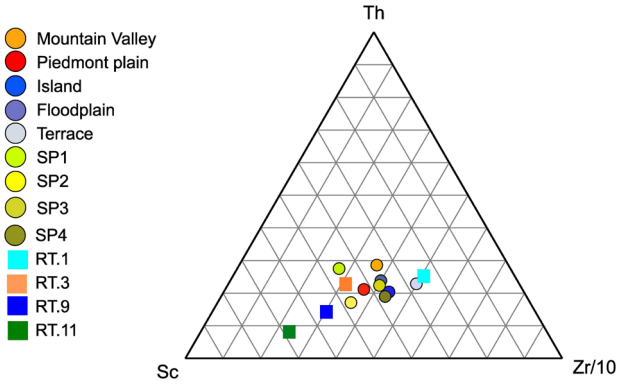


Figure 8 - Ternary diagram (Th-Sc-Zr/10) showing the composition of potential source rocks from various channel features in the Serio River.

DISCUSSION

Downstream Sediment Evolution

The sedimentary and geomorphological evolution of the Serio catchment is the result of a complex interplay between fluvial processes, chemical and physical weathering, provenance mixing, environmental forcing, and anthropogenic modifications. The Serio River has undergone substantial check-dam construction, hydropower development, channel engineering and gravel mining extraction. Characterization of sediments within the catchment provides insight into these processes through the integration of downstream trends in grain size, coarse-fraction distribution, sand-fraction lithology, geochemistry, and channel morphology.

Grain-size distributions generally show downstream fining from the mountain catchment towards the piedmont plain, reflecting progressive fining and sediment sorting

during transport. However, this natural trend is locally modified by anthropogenic influences, including check dams and channel engineering, which disrupt sediment connectivity and flow regimes. Modal grain size decreases in the mountain catchment (CB.4, 148 μm) but increases downstream in piedmont channel bed deposits (CB.14, 384 μm; table S2), suggesting local reworking and storage of coarse sediment. Finer fractions dominate low-energy settings, such as channel banks at SP1, with modal sizes around 5 μm and sand proportions as low as ~6%, while mid channel island sediments exhibit decreased sand (~27%) and increased silt (~69%). Similar textural patterns are observed in floodplain and terrace deposits.

The image-based coarse-fraction analysis demonstrates that coarse-sediment distribution is strongly influenced by local channel morphology and hydraulic conditions. As such, although we do not have coarse-grain data for multiple sites downstream, our data from Site 1 complements the downstream trend in finer grain-size. Coarser sediments are concentrated on channel bars and vegetated island margins, whereas finer coarse fractions occur within low-flow and dry channels, reflecting local variations in flow competence and sediment sorting across the active channel. Despite this pronounced lateral variability, D50 values remain predominantly within the pebble size class, indicating that the channel bed is consistently fine gravel dominated while local hydraulic conditions control the distribution and deposition of coarser and finer fractions. Although based on a single channel transect which we consider to be representative of the piedmont zone, the coarse-fraction analysis provides evidence that supports the downstream sedimentological trends identified from the bulk sediment analyses. Future investigations incorporating additional channel cross-sections would further improve understanding of the spatial variability of coarse-sediment distribution and its relationship with channel evolution.

Weathering indices indicate generally low to moderate chemical weathering throughout the Serio catchment. Channel bank deposits exhibit the highest WIC values (~83%) and Al_2O_3/CaO ratios (~25), reflecting enhanced chemical weathering and selective carbonate leaching during prolonged sediment storage. Terrace deposits also show relatively high weathering signatures, whereas floodplain and island sediments record lower values, probably owing to shorter residence times and more frequent sediment reworking. These patterns indicate that weathering intensity is controlled by the interaction of catchment lithology, sediment residence time, transport processes, and depositional environment.

Sediment lithology further reflects these controls. Serio River deposits are dominated by lithic fragments, with minor quartz and feldspar. Mountain-valley sediments are largely non-carbonate in the upper basin, whereas sediments in the middle and lower basin are predominantly carbonate-rich, with terraces, islands, and floodplains also showing elevated carbonate content. Metamorphic and volcanic clasts are abundant not only in the valley channel bed deposits, but remain well represented downstream in the piedmont plain, indicating continued sediment supply from upstream crystalline source areas despite increasing carbonate contributions.

The major element compositions reinforce the patterns observed in sediment texture, lithology, and weathering. High SiO_2 and Al_2O_3 contents in mountain catchment channel bed sediments indicate a strong silicate contribution, while elevated MgO and CaO in island and piedmont channel deposits reflect carbonate inputs and downstream accumulation. Systematic variations in SiO_2, CaO, and MgO along the transect at Site 1 highlight sediment sorting and selective transport. Collectively, these results demonstrate that sediment composition and weathering patterns in the Serio River are controlled by the interaction of catchment lithology, geomorphic setting, sediment transport, and anthropogenic modification.

Differences between channel and river bank deposits

Channel bed and river bank deposits in the Serio River display clear contrasts in sedimentological, compositional, and geochemical characteristics, reflecting differences in transport dynamics and depositional environments. In the Serio River, channel bed sediments (<2 mm) are generally coarser, more heterogeneous, and dominated by mixed siliciclastic-carbonate lithologies, with significant contributions from metamorphic and volcanic fragments in the upstream reaches. By contrast, channel bank deposits are finer-grained, with mean grain sizes decreasing to ~16 μm at the channel-bank surface, and show a vertical increase in grain size with depth, indicating progressive deposition and burial. Lithologically, channel bank profiles are enriched in carbonate components, particularly dolostone and limestone in the upper layers, while deeper sections show increased contributions from crystalline lithic fragments. Geochemically, channel bank deposits exhibit stronger weathering signatures, with increased WIC and Al_2O_3/CaO ratios in the surface layers. This pattern likely reflects longer sediment residence times and post-depositional alteration, but may also partly result from the reworking and deposition of previously weathered material derived from upstream sources or from upper channel-bank erosion. By contrast, channel bed sediments retain more primary geochemical signatures associated with active sediment transport and continuous sediment supply.

The coarse-fraction analyses show that the present-day channel bed surface is dominated by pebble-sized particles, with locally abundant cobbles and occasional isolated boulders, particularly on channel bars and vegetated island margins. Similar coarse-grained characteristics are

observed in the exposed basal gravel layer of the channel banks, which is composed predominantly of pebbles with scattered cobbles within a sandy-gravelly matrix. In contrast, the overlying channel-bank deposits are dominated by fine-grained sediments. This correspondence suggests that the basal gravel layer represents a former coarse channel deposit preserved beneath younger overbank sediments. Overall, these differences highlight that channel bed deposits primarily reflect active sediment transport and source variability, whereas channel bank deposits record sediment storage, selective deposition of fine material, and enhanced weathering.

The Serio profiles: evolution over time

The morphological evolution observed at the analyzed sites of the Serio River reflects a multi-phase adjustment of the fluvial system over the last century, with a major turning point occurring during the mid-20th century (around the 1950s). Since this period, the river has undergone progressive changes in channel form, including incision, narrowing, and subsequent phases of lateral migration, which have influenced sedimentological and grain-size characteristics in both overbank and channel facies.

At Site 1, samples collected from the bank profile (SP1) and from the present floodplain (sample CIP3) contain buried gravels which can be attributed to the active channels of 1889 and 1954 (fig. 3C). The geomorphological evolution of the active channel influenced the relative position of SP1 and CIP3 with respect to the main channel. In fact, both samples were located on the floodplain formed in 1976 (fig. 3D). Following the bed-level incision that occurred after 1976, sample SP1 remained suspended a few meters above the channel (fig. 3E). Since 2012, bank erosion processes have exposed the sediments of SP1, which form part of the present channel bank (figs 3F-H). Sample CIP3 remained part of the active channel until 1997 and has been located on a recently formed floodplain since 2000 (figs 3F-H).

At Site 2, samples CT1, CT2, CT3, and CB.14 were located within the active channels in 1889 and 1954 and on the floodplain in 1976. Subsequently, due to channel incision, they remained suspended on a terrace approximately 4 m above the current channel. Bank erosion processes between 2012 and 2015 exposed the sediments of sample CB.14 along the channel bank.

At Site 3, sample SP2 was part of the active channel in 1889 and 1954, while SP3 belonged to the active channel in 1889. Similarly, to samples CT1, CT2, and CT3 at Site 2, samples SP2 and SP3 remained suspended on terraces due to channel incision and narrowing until 2012, when bank erosion processes caused their exposure along the river banks.

At Site 4, the gravels of sample SP4 were deposited on the point bar of a meander in 1954. Between 1976 and 1988, they remained buried by finer sediments on a terrace. Starting from 1997, however, they became exposed due to lateral channel migration processes.

The channel bank profiles of the Serio River record an evolution in sediment composition that reflects changes in fluvial dynamics and geomorphological adjustment over time. Vertical variations in lithological composition within the profiles indicate a transition from older, coarser, and more crystalline-rich deposits at depth to finer, more carbonate-rich sediments in the upper layers. At several profiles (e.g., SP1 and SP3), deeper units contain higher proportions of metamorphic and volcanic lithic fragments, suggesting stronger upstream sediment supply and higher-energy transport conditions in the past. By contrast, the upper layers are dominated by dolostone and limestone, together with finer grain sizes, reflecting lower-energy overbank depositional conditions. This does not indicate a reduction in overall channel energy, but rather a shift in depositional setting, with sediments deposited outside the active channel, where local carbonate sources and finer materials are more prominent.

These compositional trends are consistent with the geomorphological evolution derived from orthophoto analysis (fig. 9). The progressive channel narrowing and incision observed between the late 19th century and the late 20th century likely enhanced vertical erosion and the reworking of older channel deposits, which are now preserved in the lower parts of the profiles. Subsequent lateral channel migration and episodic widening, particularly after the 1990s, promoted bank erosion and overbank deposition during major flood events. These processes contributed to the accumulation of finer, carbonate-rich sediments in the upper profile sections. Therefore, the Serio profiles show a transition from earlier high-energy conditions with active sediment transport to more recent phases dominated by lateral channel movement, sediment storage, and flood-related deposition, consistent with observed channel stability and periodic morphological changes over time. Finally, the reconstructed evolutionary trajectory of the Serio River – characterized primarily by channel incision and narrowing from the late nineteenth century to the 1990s – was likely driven by alterations in sediment supply and flow regime resulting from anthropogenic activities. This is consistent with observations from other Alpine rivers (Ziliani *et al.*, 2012; Scorpio and Piégay, 2021; Brenna *et al.*, 2026). These activities, including intensive gravel mining, check-dam construction, bank protection works, and levee construction, substantially modified channel processes throughout the twentieth century. In contrast, the more recent channel evolution since the 1990s, marked by a reduction in incision and narrowing, is likely associated with the cessation of gravel mining in the late 1980s and the decline in channel engineering works.

The cross-section transects and very recent history

The cross-sectional transect at Site 1 (fig. 3) of the Serio River provides key insights into very recent channel dynamics and sediment redistribution processes, particularly in relation to flood events such as occurred on November 26, 2002, October 30, 2013, and October 28, 2018. Observations within the active channel indicate a highly dynamic system characterized by alternating areas of lateral erosion, bank retreat and island erosion, and zones with deposition, channel exit and formation of new floodplains (fig. 9). Channel bed sediments are generally coarser and more heterogeneous, reflecting active transport and frequent reworking under high-energy flow conditions. By contrast, adjacent channel bank deposits consist predominantly of finer-grained material, indicating lower-energy environments where suspended sediments settle during waning flow stages or overbank flooding.

The island deposits within the transect are particularly indicative of recent geomorphological activity and are likely associated with water depth fluctuation. These deposits are dominated by fine-grained sediments (e.g., ~14 µm with high relative abundance), suggesting rapid deposition from suspension during overbank flow or periods of floodplain inundation when water spreads beyond the active channel. The formation and partial reworking of these islands correspond with the documented phases of channel widening and bank erosion observed in orthophotos following major flood events (fig. 9). Such events promote sediment redistribution across the channel, leading to the temporary stabilization with vegetation of mid channel bars or islands that may later be re-eroded or reshaped.

From a sedimentological perspective, clear contrasts exist between channel bed and channel bank environments along the transect. Channel bed sediments retain higher sand proportions and more variable lithological compositions, including both carbonate and non-carbonate lithic fragments, reflecting mixed provenance and continuous sediment supply. In contrast, channel bank and overbank deposits show increased proportions of silt and clay, enrichment in carbonate fractions (particularly dolostone and limestone), and stronger weathering signatures, indicating longer residence times and post-depositional alteration.

Overall, the cross-section transect captures a snapshot of an actively adjusting fluvial system, where recent flood events, play a major role in shaping channel morphology, redistributing sediments, and controlling the spatial variability of sedimentological properties across channel bed, island, and bank environments.

CONCLUSION

This study demonstrates that the sedimentological characteristics of the Serio River record the combined effects of sediment supply, transport processes, depositional environment, and anthropogenic river modification. Natural processes produce characteristic downstream fining, variations in sediment composition, and morphological adjustments driven by episodic floods, while sediment transport, storage, and residence time control grain-size distributions, lithological composition, and geochemical signatures along the river continuum.

The Serio River illustrates how these natural processes are further modified by human interventions, particularly check-dam construction and channel engineering. Channel bed sediments primarily record active transport and mixed provenance, whereas channel bank deposits contain finer material with stronger weathering signatures, reflecting longer residence times and post-depositional alteration. Vertical profiles reveal a temporal evolution from older, coarse, crystalline-rich deposits at depth to younger, finer,

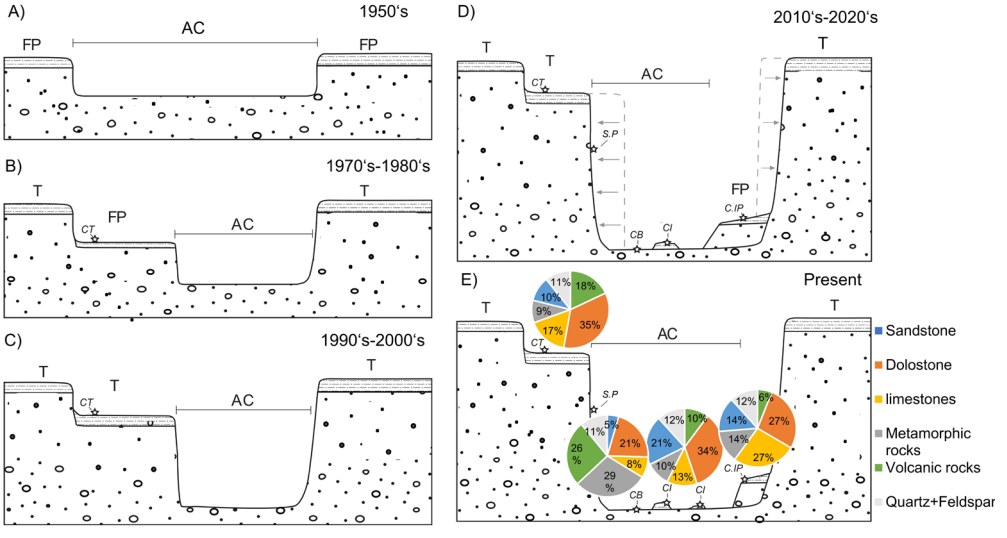


Figure 9 - Evolution of the Serio channel in the piedmont plain from 1950 to the Present (A-E), gross sand composition of the four main landforms is reported in the present (E).

carbonate-rich sediments near the surface. These trends correspond with geomorphological evidence of channel narrowing, incision, lateral migration, and episodic morphological adjustments linked to flood events, highlighting the close relationship between channel evolution and sediment characteristics.

Overall, this study shows that recent channel adjustment in the Serio River is recorded by systematic downstream and vertical changes in sediment properties. Variations in grain size, lithological composition, geochemistry, and weathering indices demonstrate how river regulation has modified sediment transport, storage, and depositional patterns while preserving evidence of both natural and anthropogenic controls within the sedimentary record.

ABBREVIATION LIST:

CB: Channel bed grain of Serio river
CI: Channel Island of Serio river
CT: Channel Terrace of Serio river
C.IP: Channel flood plain of Serio river
CE TOT: Carbonate total
L-CE TOT: Lithic without Carbonate total
Q+F: Quartz and Feldspar
SP1: Serio river bank profile 1
SP2: Serio river bank profile 2
SP3: Serio river bank profile 3
SP4: Serio river bank profile 4

SUPPLEMENTARY MATERIALS

Supplementary material associated to this article including 9 figures and 4 tables can be found in the online version at https://doi.org/10.4454/j3c5gh52

AUTHORS CONTRIBUTION

Conceptualization: Q.I, K.F; Methodology: Q.I, K.F; Data Collection, Curation, Analysis and Validation: Q.I, S.P, V.S, G.M, T.L, K.F; Writing original draft: Q.I ; Review & Editing: K.F, C.Z, K.M, V.S, G.M, S.P; Funding acquisition: Q.I, K.F; Project administration, resources, software: Q.I, K.F, K.M, C.Z, T.L. Supervision: K.F, C.Z. All authors have read and agreed to the published version of the manuscript.

ACKNOWLEDGMENTS

This research was supported by the University of Central Asia (UCA) and the German Academic Exchange Service (DAAD). The authors also acknowledge the University of Tübingen for providing institutional infrastructure, research facilities, and administrative support during the study. We are grateful to Dr. Andrea Aquino for his assistance with thin-section preparation, Dr. Sandro Rossato for his support during the fieldwork campaign, and Dr. Amin Ghafarpour for his valuable initial feedback on the geochemical aspects of this study. This work was performed within the framework of the "Convenzione di collaborazione per l'analisi geomorfologica del Fiume Serio finalizzata alla sua gestione integrata e sostenibile", funded by Autorità di Bacino Distrettuale del Fiume Po.

REFERENCES

Albano R., Mancusi L., Abbate A., 2017. *Improving flood risk analysis for effectively supporting the implementation of flood risk management plans: The case study of "Serio" Valley*. Environmental Science and Policy, 75, 158-172. https://doi.org/10.1016/j.envsci.2017.05.017

ARPA, 2025. *SIDRO - Sistema Informativo Idrogeologico*. ARPA Lombardia. https://idro.arpalombardia.it/it/map/sidro/

Brenna A., Bizzi S., Surian N., 2026. *The great decline of suspended sediment load in the Po River (Italy) over the last 100 years*. Catena, 265, 109864. https://doi.org/10.1016/j.catena.2026.109864

Canobbio S., Mezzanotte V., Benvenuto F., Siotto M., 2010. *Determination of Serio River (Lombardy, Italy) ecosystem dynamics using macroinvertebrate functional traits*. Italian Journal of Zoology, 0003. https://doi.org/10.1080/11250000903183600

Cavalleri F., Lussana C., Viterbo F., Brunetti M., Bonanno R., Manara V., Lacavalla M., Sperati S., Raffa M., Capecchi V., Cesari D., Giordani A., Maria I., Cerenzia L., Maugeri M., 2024. *Multi-scale assessment of high-resolution reanalysis precipitation fields over Italy*. Atmospheric Research, 312, 107734. https://doi.org/10.1016/j.atmosres.2024.107734

Comiti F., 2012. *How natural are Alpine mountain rivers? Evidence from the Italian Alps*. Earth Surface Processes and Landforms, 37 (7), 693-707. https://doi.org/10.1002/esp.2267

Comiti F., Da Canal M., Surian N., Mao L., Picco L., Lenzi M.A., 2011. *Channel adjustments and vegetation cover dynamics in a large gravel bed river over the last 200 years*. Geomorphology, 125 (1), 147-159. https://doi.org/10.1016/j.geomorph.2010.09.011

Cucchiaro S., Martini L., Maset E., Pellegrini G., Eliana M., Beinat A., Cazorzi F., Picco L., 2024. *Multi-temporal analysis to support the management of torrent control structures*. Catena, 235, 107599. https://doi.org/10.1016/j.catena.2023.107599

Demurtas L., Bruno L., Lugli S., Fontana D., 2022. *Evolution of the Po-Alpine River System during the Last 45 Ky Inferred from Stratigraphic and Compositional Evidence (Ostiglia, Northern Italy)*. Geosciences (Switzerland), 12 (9). https://doi.org/10.3390/geosciences12090342

Demurtas L., Fontana D., Lugli S., Bruno L., 2024. *Multi-source detrital contributions in the Po alluvial basin (northern Italy) since the Middle Pleistocene. Insights into sediment accumulation in intermediate sinks*. Basin Research, 36 (1), 1-20. https://doi.org/10.1111/bre.12858

Folk R.L., 1980. *Petrology of sedimentary rocks*. Hemphill Publishing Company, Austin (TX).

Fontana A., Mozzi P., Marchetti M., 2014. *Alluvial fans and megafans along the southern side of the Alps*. Sedimentary Geology, 301, 150-171. https://doi.org/10.1016/j.sedgeo.2013.09.003

Garzanti E., 2016. *From static to dynamic provenance analysis. Sedimentary petrology upgraded*. Sedimentary Geology, 336, 3-13.

Garzanti E., Andò S., Vezzoli G., 2006. *The continental crust as a source of sand (Southern Alps cross section, northern Italy)*. The Journal of Geology, 114 (5), 533-554.

Garzanti E., Vezzoli G., Andò S., 2011. *Earth-Science Reviews Paleogeographic and paleodrainage changes during Pleistocene glaciations (Po Plain, Northern Italy).* Earth Science Reviews, 105 (1-2), 25-48. https://doi.org/10.1016/j.earscirev.2010.11.004

Govindaraju K., 1989. *Compilation of working values and sample description for 272 geostandards*. Sedimentary Geology, 13, 1-113. https://doi.org/https://doi.org/10.1111/j.1751-908X.1989.tb00476.x

Ingersoll R. V, Bullard T.F., Ford R.L., Grimm J.P., Pickle J.D., Sares S.W., 1984. *The effect of grain size on detrital modes: a test of the Gazzi-Dickinson point-counting method*. Journal of Sedimentary Research, 54 (1), 103-116.

Isotta F.A., Frei C., Weilguni V., Perčec Tadić M., Lassegues P., Rudolf B., Pavan V., Cacciamani C., Antolini G., Ratto S.M., 2014. *The climate of daily precipitation in the Alps: development and analysis of a high-resolution grid dataset from pan-Alpine rain-gauge data*. International Journal of Climatology, 34 (5), 1657-1675.

Jan G., Eynatten H. von, 2004. *Quantitative provenance analysis of sediments: review and outlook*. Sedimentary Geology, 171, 1-11. https://doi.org/10.1016/j.sedgeo.2004.05.007

Liu Y., Liu X., Sun Y., 2021. *QGrain: An open-source and easy-to-use software for the comprehensive analysis of grain size distributions*. Sedimentary Geology, 423, 105980. https://doi.org/10.1016/j.sedgeo.2021.105980

Llena M., Vericat D., Cavalli M., Crema S., Smith M.W., 2019. *The effects of land use and topographic changes on sediment connectivity in mountain catchments*. Science of the Total Environment, 660, 899-912. https://doi.org/10.1016/j.scitotenv.2018.12.479

Marchi L., Comiti F., Crema S., Cavalli M., 2019. *Channel control works and sediment connectivity in the European Alps*. Science of the Total Environment, 668, 389-399. https://doi.org/10.1016/j.scitotenv.2019.02.416

McLennan S.M., 1993. *Weathering and global denudation*. The Journal of Geology, 101 (2), 295-303.

Ménégoz M., Valla E., Jourdain N.C., Blanchet J., Beaumet J., Wilhelm B., Gallée H., Fettweis X., Morin S., Anquetin S., 2020. *Contrasting seasonal changes in total and intense precipitation in the European Alps from 1903 to 2010*. Hydrology and Earth System Sciences, 5355-5377.

Microtrac Retsch GmbH, 2023. *Microtrac particle characterization*. Microtrac. https://www.microtrac.com/

Nesbitt H.W., Young G.M., 1982. *Early Proterozoic climates and plate motions inferred from major element chemistry of lutites*. Nature, 299 (5885), 715-717.

Piasecka J., Święchowicz J., Najwer A., Zwoliński Z., 2025. *Impact of the Water Reservoir and River Engineering Structures on Longitudinal and Transverse (Dis) connectivity Associated with Sediment Transfer.* Land Degradation & Development, 2609-2638. https://doi.org/10.1002/ldr.5519

Piton G., Carladous S., Recking A., Tacnet J.M., Liébault F., Kuss D., Quefféléan Y., Marco O., 2016. *Why do we build check dams in Alpine streams? An historical perspective from the French experience*. Earth Surface Processes and Landforms, 108, 91-108. https://doi.org/10.1002/esp.3967

Pittau S., Scorpio V., 2026. *Geomorphology Effects of sediment connectivity changes on channel evolutionary trajectory: the case study of the Taro and Ceno rivers in the Northern Apennines (Italy).* Geomorphology, 495, 110131. https://doi.org/10.1016/j.geomorph.2025.110131

Ravazzi C., Deaddis M., Amicis M. De, Marchetti M., Vezzoli G., Zanchi A., 2012. *The last 40 ka evolution of the Central Po Plain between the Adda and Serio rivers*. Géomorphologie: relief, processus, environnement, 18 (2), 131-154.

Regione Lombardia, 2024. *Historical Archive of Regione Lombardia* [Accessed January 2024]

Sanderson D.C.W., Murphy S., 2010. *Using simple portable OSL measurements and laboratory characterization to help understand complex and heterogeneous sediment sequences for luminescence dating.* Quaternary Geochronology, 5 (2-3), 299-305. https://doi.org/10.1016/j.quageo.2009.02.001

Schneider C.A., Rasband W.S., Eliceiri K.W., 2012. *NIH Image to ImageJ: 25 years of image analysis*. Nature methods, 9 (7), 671-675.

Schulte P., Sprafke T., Rodrigues L., Fitzsimmons K.E., 2018. *Are fixed grain size ratios useful proxies for loess sedimentation dynamics? Experiences from Remizovka, Kazakhstan*. Aeolian Research, 31, 131-140. https://doi.org/10.1016/j.aeolia.2017.09.002

Scorpio V., Andreoli A., Zaramella M., Moritsch S., Theule J., Agnese A.D., 2020. *Restoring a glacier-fed river: past and present morphodynamics of a degraded channel in the Italian Alps.* Earth surface processes and landforms, 2823, 2804-2823. https://doi.org/10.1002/esp.4931

Scorpio V., Comiti F., Rinaldi M., Surian N., 2024a. *Channel changes over the last 200 years: A meta data analysis on European rivers*. Earth surface Processes and Landforms, 2651-2676. https://doi.org/10.1002/esp.5848

Scorpio V., Crema S., Marra F., Righini M., Ciccarese G., Borga M., Cavalli M., Corsini A., Marchi L., 2018. *Science of the Total Environment Basin-scale analysis of the geomorphic effectiveness of flash floods: a study in the northern Apennines (Italy).* Science of the Total Environment, 640-641, 337-351. https://doi.org/10.1016/j.scitotenv.2018.05.252

Scorpio V., Marchese E., Comiti F., Coviello V., Gems B., Vignoli G., 2024b. *Multi-decadal quantification of interactions between coarse sediment fluxes and channel management in South Tyrol, Eastern European Alps General characteristics*. Earth Surface Processes and Landforms, 1869-1889. https://doi.org/10.1002/esp.5804

Scorpio V., Piégay H., 2021. *Is afforestation a driver of change in Italian rivers within the Anthropocene era?* Catena, 198, 105031.

Surian N., Mao L., Giacomin M., Ziliani L., 2009. *Morphological effects of different channel- forming discharges in a gravel-bed river.* Earth Surface Processes and Landforms, 1107, 1093-1107. https://doi.org/10.1002/esp

Surian N., Righini M., Lucía A., Nardi L., Amponsah W., Benvenuti M., Borga M., Cavalli M., Comiti F., Marchi L., Rinaldi M., Viero A., 2016. *Geomorphology Channel response to extreme floods: insights on controlling factors from six mountain rivers in northern Apennines, Italy*. Geomorphology, 272, 78-91. https://doi.org/10.1016/j.geomorph.2016.02.002

Viganò G., Confortola G., Fornaroli R., Ph D., Cabrini R., Canobbio S., Ph D., 2013. *Effects of Future Climate Change on a River Habitat in an Italian Alpine Catchment*. Journal of Hydrologic Engineering, 1-14. https://doi.org/10.1061/(ASCE)HE.1943-5584.0001293.

Wang X., Wei H., Khormali F., Taheri M., Kehl M., Frechen M., Lauer T., Chen F., 2017. *Grain-size distribution of Pleistocene loess deposits in northern Iran and its paleoclimatic implications*. Quaternary International, 429, 41-51. https://doi.org/10.1016/j.quaint.2016.01.058

Ziliani L., Surian N., 2012. *Geomorphology Evolutionary trajectory of channel morphology and controlling factors in a large gravel-bed river.* Geomorphology, 173-174, 104-117. https://doi.org/10.1016/j.geomorph.2012.06.001

(Ms. received 30 April 2026, accepted 31 July 2026)